

Enhanced ductility and fracture classification maps for advanced high-strength steels considering local ductility and fracture toughness

David Frómeta^{1*}, Laura Grifé¹, and Daniel Casellas¹

¹Eurecat, Centre Tecnològic de Catalunya, Unit of Metallic and Ceramic Materials, 08243 Manresa, Spain

Abstract. Alternative classification diagrams considering global and local ductility have been introduced recently in order to better describe the overall formability of advanced high-strength steels (AHSSs). These diagrams combine different parameters obtained from uniaxial tensile tests to rank steel formability and establish objective performance indicators. However, such classification schemes may fail to estimate fracture performance in certain failure modes related to the material's damage tolerance and crack propagation resistance, which is fundamental for a safe implementation of high-strength steels in structural and safety related applications. The present work proposes a new classification concept for AHSSs, considering not only global and local ductility but also fracture toughness. The proposed criteria aim to provide a more comprehensive definition of AHSSs formability and cracking resistance, considering intrinsic material parameters. Different strain- and energy-based parameters are analysed and their relevance to material ranking is discussed. The study is based on the analysis of 25 AHSSs, including Dual Phase, Complex Phase, TRIP, TRIP-aided Bainitic Ferritic, Press hardened steels, Quenching&Partitioning and Medium-Mn steels with tensile strengths ranging from 800 to 1500 MPa.

Keywords: Advanced High Strength Steels; Global ductility; Local ductility; fracture toughness

1 Introduction

The automotive industry faces increasingly demanding challenges driven by cost competitiveness, sustainability and circular economy policies. From a materials perspective, steel remains the most cost-effective and sustainable solution for manufacturing high-performance body and chassis automotive products. This is in great part thanks to the continuous advances in steel research and innovation, which have led to the development of new advanced steel solutions capable of meeting the strict quality and safety standards of the automotive industry at affordable costs.

A clear example of this is the advent of the so-called Advanced High Strength Steels (AHSSs) family. AHSSs are sophisticated materials characterized by complex multi-phase microstructures that provide unique combinations of strength and ductility. Their higher strength and enhanced impact performance compared to conventional steels allow for reducing the weight of structural and safety-related components while improving the protection of the occupants.

All these facts together with the affordability of the manufacturing processes, are the key reasons that have motivated the widespread adoption of AHSSs in passenger's cars. However, the implementation of these new high-performance steels has evidenced different challenges and limitations, mostly related to their higher cracking susceptibility and the difficulty of predicting certain types of failure, such as sheared edge fracture, using conventional ductility and formability approaches based on elongation values from uniaxial tensile tests and Forming Limit Curves (FLCs).

This has made it necessary the definition of new material metrics for a more accurate classification of AHSS formability and fracture resistance of AHSSs. Recently, many research works have focused on the distinction between global and local formability and have proposed different parameters obtained from standard uniaxial tensile tests to describe both [1-5].

Global formability refers to the material's resistance against the formation of localized necking. It is used to define deformation modes where relatively large regions of material are deformed simultaneously (stretch forming, drawing, etc.) and strain localization occurs due to the application of a uniform deformation. Global formability can be described by uniaxial tensile parameters (true uniform strain, elongation at fracture, n -value) and FLCs. The FLC defines the deformation limits of a material for multiple strain paths, represented by different combinations of principal strains. These critical strains represent the onset of localized necking and determine the limits below which safety margins for sheet metal forming are calculated. The FLC is experimentally evaluated according to ISO 12004-1. It requires testing several Nakajima or Marciniak samples with different geometries to obtain deformation paths between uniaxial and equi-biaxial tension.

Due to the large amount of material needed and the complexity of the experimental setup for FLC determination, other parameters from uniaxial tensile tests, such as the true uniform strain (ϵ_u) and the strain hardening exponent (n), are often used as a simplified measure of global formability. Both ϵ_u and n inform about the material's ability to uniformly distribute in-plane deformation.

* Corresponding author: david.frometa@eurecat.org

Local formability, on the other hand, is defined as the ability of a material to undergo plastic deformation in a local area without fracture [2]. It can be measured by local fracture strain measurements and represented in the principal strain space in the form of Fracture Forming Limit Lines (FFLs) or plotting fracture strains as a function of stress triaxiality [6]. Alternatively, parameters like the True Thickness Strain (TTS) [1, 2] or the True Fracture Strain (TFS) [3-5] obtained from uniaxial tensile tests may effectively provide a qualitative estimation of local formability, without the need of excessive testing and complex experimental procedures.

A particular case of local formability is sheared edge formability. In this case, the material to be formed has been damaged in a previous shearing or punching operation and, thus, its stretching capacity is limited. Sheared edge formability of sheet metallic materials is generally represented by the ISO 16630 Hole Expansion Ratio (HER). However, this parameter is not an intrinsic material property and depends on many factors that can compromise its reliability [7,8]. Accordingly, the use of more intrinsic material parameters, such as the TTS or the TFS, are being used preferentially over the HER to local formability ranking and microstructural design guidance.

Other authors have emphasized the role of the material's crack propagation resistance on the sheared edge formability of AHSS. Denks et al. [4] showed that local ductility, as measured by the TFS, was not enough to explain the punched hole expansion capacity of hot-rolled steel grades and introduced the term *crack resistivity*. This parameter, defined as the maximum local fracture strain at shear edges stretched using a Nakajima setup, showed much better correlation with HER than the TFS.

The work of Frómata et al. [9] showed an excellent correlation between fracture toughness, measured in terms of essential work of fracture (w_e), and HER. This correlation was attributed to the similarity in fracture mechanisms governing punched edge formability and fracture mechanics tests. The same parameter, w_e , was used in [10] to rank the crash fracture performance of several AHSSs and PHSSs, which is another local ductility related failure mode. The investigations showed that the crash failure of these steels is dominated by the formation and propagation of cracks through the material, which explains that steels with superior fracture toughness exhibit enhanced crash performance. These observations show the relevance of fracture toughness, the essential work of fracture in particular, for AHSS formability and fracture performance ranking.

This paper explores different ductility and fracture performance classification maps based on some of the global/local ductility and fracture toughness concepts mentioned above for a wide range of AHSS. Several intrinsic material parameters are used as a qualitative measure of global and local formability. The proposed diagrams aim at providing alternative classification schemes for a more objective and accurate description of AHSS formability and fracture performance. These schemes can be valuable for the development of new

steel grades and for application-oriented material selection.

2 Methods and procedures

2.1 Materials

A total of 25 AHSS grades are considered in this study, including, Dual Phase (DP), Complex Phase (CP), TRIP, TRIP-aided Bainitic Ferritic (TBF), Press hardened steels (PHS), Quenching&Partitioning (Q&P) and Medium-Mn (MMn) steels. Basic mechanical properties for the analysed steel grades are given in Table 1. Most of the mechanical properties are retrieved from previously published research [9-12]. For more details about microstructural characteristics and other relevant information, please refer to the original publication.

Table 1. Mechanical properties of the investigated materials for the transverse direction. t = thickness, Y_S =yield stress, UTS = ultimate tensile strength, UE = Uniform elongation, TE = Total elongation at fracture.

Steel	t [mm]	Y_S [MPa]	UTS [MPa]	UE [%]	TE [%]
CP1000 [10]	1.4	915	1008	4.8	8.8
DP1000 [10]	1.4	775	1015	7	11.4
TBF [10]	1.5	755	1012	10.5	15.8
Q&P [10]	1.4	920	1202	5.3	9.1
CP1200 [10]	1.6	1041	1218	3.4	6
TBF/Q&P [10]	1.4	876	1026	7.5	11.3
PHS1500 [10]	1.5	1075	1552	3.7	5.2
PHS1000 [10]	1.5	988	1007	4.9	7.3
DP780 [9]	1.5	513	823	14.2	19.9
TRIP780 [9]	1.6	542	851	20.7	25.8
DP1000A [9]	1.35	816	1055	6.5	9.7
3Gen DP1180 [9]	1.2	895	1212	10.5	14.3
3Gen TBF1180 [9]	1.4	987	1216	9.2	12.6
3Gen Q&P1180 [9]	1.5	1034	1191	9.2	13.1
DP1000B [11]	1.4	773	1040	5.4	8.7
PHS_FB [12]	2.0	550	812	11.8	9.3
PHS_B [12]	2.0	836	971	5.1	9.5
PHS_BM [12]	2.0	1112	1728	4.1	4.8
PHS_M [12]	2.0	1167	1626	4.3	5.4
Q&P980*	1.5	658	992	14.4	19
Q&P1180*	1.66	1033	1201	12	14.7
Q&P 1200 *	1.5	1032	1214	10.7	14.9
Q&P 1400 *	1.6	1148	1396	4.9	7.4
MMn 1000 *	1.5	643	960	25.7	29.6
MMn 1270*	1.4	1078	1228	8.6	9.3

*New data

2.2 Local ductility measurements

TFS was evaluated according to Equation (1):

$$TFS = \ln \left(\frac{A_0}{A_f} \right) \quad (1)$$

where A_0 is the initial cross-section area and A_f is the area at fracture. The area at fracture was measured from the fracture surface of the tensile specimens according to ASTM E8 with an optical microscope (Fig.1).

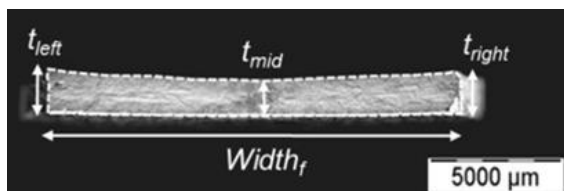


Fig. 1. Fracture surface of a uniaxial tensile specimen and location of the thickness and width measurements performed to evaluate the TFS. The dashed line represents the contour of the fractured area

2.3 Fracture toughness evaluation

The fracture toughness of all the steel grades analysed in this work was evaluated by means of the Essential Work of Fracture (EWF) methodology [13]. EWF tests were performed with fatigue pre-cracked Double Edge Notched Tension (DENT) specimens according to CWA 17793:2021 [14]. An example of the specimen geometry used for EWF tests in [9-11] is given in Fig.2a. Fig.2b and Fig.2c show a schematic representation of the experimental procedure for the evaluation of the EWF. An exhaustive description of the EWF procedure, as well as the number of specimens and ligament lengths used for the different steel grades, is available in previous works [9, 10]. In this paper, only specific essential work of fracture (w_e) values are reported. All the reported values correspond to specimens machined in the transverse orientation with respect to the rolling direction (notches aligned in the rolling direction).

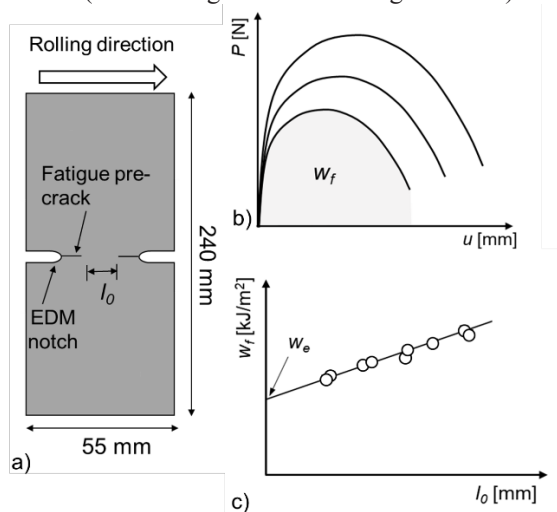


Fig. 2. a) Specimen geometry used for EWF tests; b) Load-displacement curve for DENT specimens with different ligament lengths, c) specific work of fracture (w_f) as a function of ligament length (l_0) and determination of w_e by extrapolation to zero ligament length.

3 Results and discussion

3.1 Local ductility and fracture toughness

Results from local fracture strain measurements and EWF are shown in Table 2. Values of TFS are reported when available. The data is obtained from previous works, except for the six last steel grades marked with an asterisk.

Table 2. Local ductility (TFS) and fracture toughness (w_e).

Steel	t [mm]	TFS [-]	w_e [kJ/m ²]
CP1000 [10]	1.4	1.21	405 ± 11
DP1000 [10]	1.4	0.6	138 ± 20
TBF [10]	1.5	0.64	149 ± 13
Q&P [10]	1.4	1.05	194 ± 12
CP1200 [10]	1.6	-	201 ± 24
TBF/Q&P [10]	1.4	-	302 ± 32
PHS1500 [10]	1.5	-	159 ± 11
PHS1000 [10]	1.5	-	330 ± 21
DP780 [9]	1.5	0.48	151 ± 31
TRIP780 [9]	1.6	0.49	106 ± 24
DP1000A [9]	1.35	0.57	149 ± 21
3Gen DP1180 [9]	1.2	0.49	115 ± 20
3Gen TBF1180 [9]	1.4	0.55	104 ± 30
3Gen Q&P1180 [9]	1.5	0.63	196 ± 31
DP1000B [11]	1.4	0.53	286 ± 17
PHS_FB [12]	2.0	-	189 ± 14
PHS_B [12]	2.0	-	352 ± 14
PHS_BM [12]	2.0	-	78 ± 6
PHS_M [12]	2.0	-	149 ± 16
Q&P980*	1.5	0.79	133 ± 24
Q&P1180*	1.66	0.67	111 ± 49
Q&P 1200 *	1.5	0.65	189 ± 32
Q&P 1400 *	1.6	0.77	225 ± 26
MMn 1000 *	1.5	0.96	142 ± 64
MMn 1270*	1.4	0.66	187 ± 19

*New data

3.2 AHSS classification diagrams

3.2.1 Classification according to tensile strength

Fig.3 shows the classical classification map for steels based on total elongation and tensile strength, also known as the “banana diagram”. This diagram is commonly used to classify steel grades according to their strength and ductility and provides a visual rapid description of the different steel types. In conventional steels and 1st generation AHSSs, elongation tends to gradually decrease with increasing strength, describing a banana-like shape that gives the colloquial name to the plot. However, new AHSS families, like 3rd Generation AHSSs, including TRIP-assisted, Q&P and Medium-Mn steels provide unusual combinations of strength and ductility that make this designation no longer appropriate.

An alternative diagram plotting w_e , instead of TE, as a function of tensile strength is shown in Fig.4. This diagram was proposed in [9] to classify AHSSs according to their cracking resistance. It is interesting to note that the arrangement of steel families can be completely different when compared to the traditional strength-ductility plot. It is especially notable the large differences for Medium Mn steel, which exhibits extraordinary elongation for its strength level. However, when looking at fracture toughness properties, the Medium Mn steel can be grouped with steels lying in the moderate-to-low range of crack propagation resistance (DP/TRIP/TBF). The opposite occurs for CP steels, which have modest elongation values but very high fracture toughness. Such large differences in ductility and fracture toughness stress the importance of not

trusting elongation values for fracture resistance estimation since completely wrong assumptions can be made.

This fact generates a new paradigm, where local ductility and crack propagation resistance take on greater importance and become essential parameters to guide microstructural design and improve material selection.

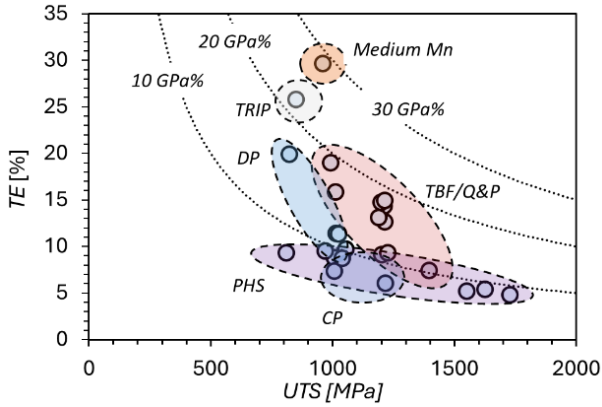


Fig. 3. Total elongation vs Ultimate Tensile Strength

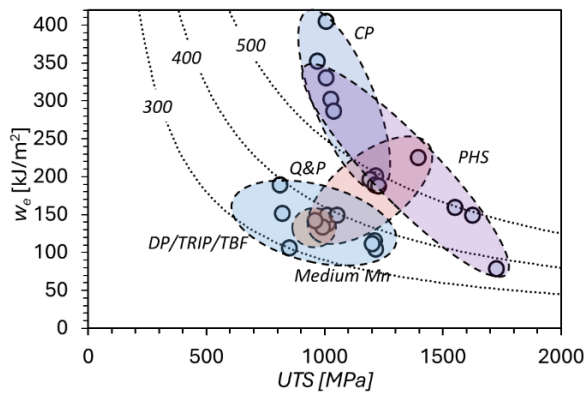


Fig. 4. Fracture toughness vs Ultimate Tensile Strength

3.2.2 Local vs global ductility

The steel grades analysed in this study are represented in Fig.5 using the local/global ductility diagram proposed by Hance [3]. The plot offers a better description of the formability performance considering the positioning of the steels. Different classification and rating parameters are defined. The local/global strain ratio (TFS/ϵ_u) indicates the balance between local and global formability. On the other hand, the formability index (F.I. see description in Table 3), provides an estimate of the overall formability, considering both global and local formability.

According to this diagram, differences in global and local formability can be observed for the different steel families. On the one hand, CP steel possesses a very good local ductility and it is rated with “good” overall formability according to the F.I. On the other hand, DP/TRIP/TBF steels are positioned in the balanced/global ductility region. Q&P steels tend to exhibit similar global formability to TBF steels but slightly superior local ductility. The Medium Mn steel

shows exceptional global and local ductility and it is rated “excellent” based on the F.I.

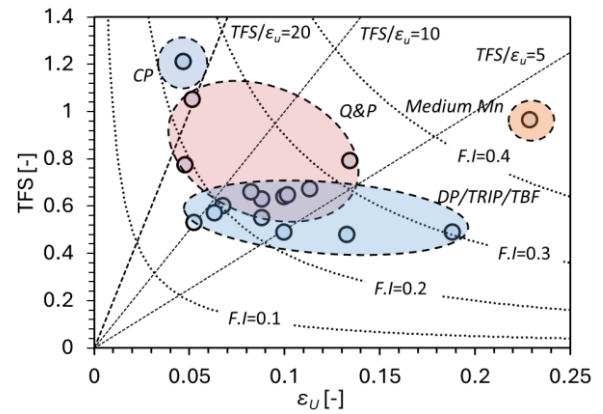


Fig. 5. Local vs global formability. F.I.: Formability Index

Table 3. Performance parameters obtained from uniaxial tensile and EWF tests

Parameters	Definition
Local/Global strain ratio [3]	TFS/ϵ_u
Formability Index (F.I) [3]	$\sqrt{\epsilon_u \cdot TFS}$
Performance Index (P.I.) [3]	$UTS \cdot \sqrt{\epsilon_u \cdot TFS}$
Global toughness [5]	$\frac{1}{2} (YS+UTS)e_t$
Toughness Index (T.I)	$\sqrt{w_e \cdot \left(\frac{YS + UTS}{2}\right) e_t}$
Fracture toughness/Global toughness ratio	$w_e / \left(\frac{YS+UTS}{2}\right) e_t$

3.2.3 Fracture toughness vs global ductility and toughness

The presented local/global formability diagram offers an enhanced classification system for rating the formability performance of AHSSs. However, it does not consider the crack propagation resistance of the material. As mentioned before, local ductility may not be sufficient to explain certain types of failures more intrinsically related to the material’s crack resistivity [4]. Therefore, considering crack propagation resistance may be necessary to better describe the fracture performance of AHSSs and provide a more complete description of the overall formability and cracking resistance.

Based on this argument, Frómata et al. [9] proposed an alternative performance mapping approach accounting for crack propagation resistance. Similarly to the local/global ductility plot, the diagram plots the uniform elongation in the x-axis but, instead of the TFS, w_e is represented in the y-axis. w_e has been shown to be a good indicator of edge cracking sensitivity and crash fracture performance of AHSSs [9, 10]. Therefore, it is a valuable material parameter to optimize the development and selection of AHSSs with enhanced fracture resistance and damage tolerance.

The diagram is shown in Fig.6. It is divided into different quadrants according to global ductility and cracking resistance levels. The more to the right in the plot the greater the global formability, whereas upper

quadrants indicate superior fracture resistance and damage tolerance.

Looking at this classification system, some similarities are observed compared to the local/global ductility map. First, the distribution of CP, DP/TRIP/TBF and Q&P steels is quite similar, i.e. CP shows high cracking resistance and moderated global formability, DP/TRIP/TBF show low cracking resistance and good global formability, and Q&P present a more balanced combination of global formability and cracking resistance.

Such differences can be attributed to the microstructural characteristics of multiphase AHSSs. Dual Phase-like steels (DP/TRIP/TBF) present more heterogeneous microstructures consisting of a soft ferrite/bainitic ferrite with the presence of hard secondary phases (martensite) embedded in the matrix. The strain gradients between the soft matrix and the hard secondary phases contributes to increase the strain hardening rate and to delay the onset of localized necking. Accordingly, DP-microstructures usually present higher strain hardening and elongation (both uniform and total than more homogeneous CP-like microstructures. However, the same mechanisms that contribute to enhancing global ductility may have a negative impact on local formability and fracture toughness [2, 9,15]. The hardness differences between phases generate internal stresses during deformation that contribute to the rapid generation of microvoids and/or decohesion of the ferrite/martensite interfaces. In the presence of a crack or defect, such microvoid coalescence rapidly contributes to the crack propagation and final fracture of the sample [15]. On the other hand, CP microstructures have a more moderated global ductility but are less sensitive to local failure, which results in superior local formability and fracture toughness [2, 9, 15]. In the case of Q&P steels, the combination of homogeneous bainite/tempered martensite matrix with the strain-induced transformation of retained austenite to martensite (TRIP effect) provides a good balance between global ductility and fracture toughness [9].

The most noticeable difference between local ductility and fracture toughness is found in the Medium Mn steel. In Fig.6 this steel is positioned in the low crack propagation resistance region, which contrasts with the high TFS shown in Fig.5. This fact can be related to the large volume fraction of retained austenite of this steel (around 40%). The TRIP effect contributes to significantly improve strength and ductility in uniaxial tensile tests. However, the high stress triaxiality at the crack tip promotes an increased retained austenite to martensite transformation rate that can be detrimental to crack propagation resistance due to the formation of a “brittle” network of train-induced fresh martensite ahead of the crack tip [16].

This corroborates that there is not necessarily a direct relationship between local ductility and cracking resistance [4, 9]. Therefore, for applications requiring high crack propagation resistance and damage tolerance, fracture toughness should be the most appropriate indicator for material selection.

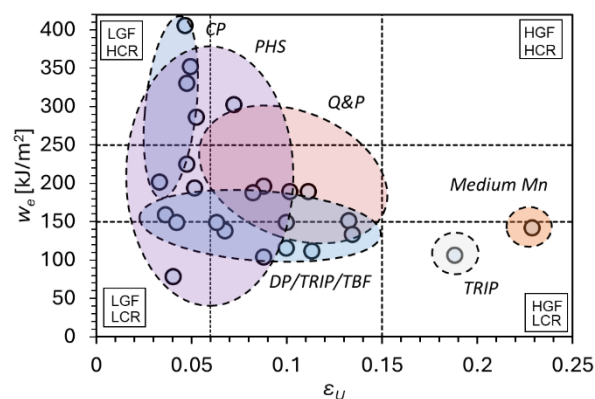


Fig. 6. Fracture toughness vs global formability. LGF: Low global formability; LCR: Low cracking resistance; HGF: High global formability; HCR: High cracking resistance.

Another classification and rating concept is shown in Fig.7. In this case, the fracture toughness is represented against the global toughness. Usually, many metallurgical researchers have used the product of the tensile strength by the total elongation (UTSXTE) from uniaxial tensile tests. A modified version of the global toughness concept was introduced by Yim et al. [5]. Instead of using UTS, they proposed the use of the average between yield strength and ultimate tensile strength multiplied by the total elongation ($1/2 (YS+UTS)e_t$). This definition is used to represent global toughness in Fig.7.

The classification scheme is similar to the one shown in Fig.5. However, two new parameters are introduced, the ratio between fracture toughness and global toughness (FT/GT) and the Toughness Index (T.I, Table 2). The greater the FT/GT ratio the greater the dominance of fracture toughness over global toughness. The T.I. provides a rating system considering an overall toughness.

Concerning steel classification. No significant differences in material ranking are observed in the fracture toughness vs global toughness diagram compared to the local vs global formability map (Fig.5)

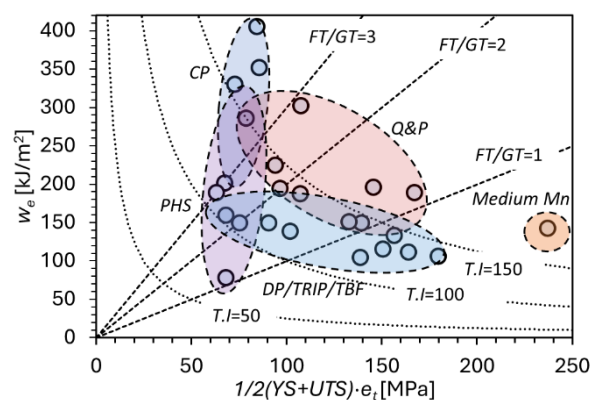


Fig. 7. Fracture toughness vs global toughness. FT: fracture toughness; GT: Global toughness

The analysis presented in this work emphasizes the need for enhanced AHSS classification concepts, considering global ductility, local ductility and fracture toughness. As it has been shown, local ductility is not always correlated to crack propagation resistance.

Therefore, fracture toughness measurements can be a valuable tool to obtain a more accurate description of the overall formability and fracture performance of AHSSs.

4 Conclusions

The present work has explored different classification schemes for AHSS formability ranking, considering global formability, local formability and fracture toughness.

The study shows that traditional steel classification maps based on tensile strength and elongation from uniaxial tensile tests are not enough to describe the local formability and fracture potential of AHSSs. Therefore, a transition from the traditional “banana diagram” to more specific and comprehensive classification diagrams is necessary.

Local vs global ductility maps offer a good classification and rating system for AHSS formability performance. However, they do not account for crack propagation resistance, which can be relevant for certain forming operations, such as sheared edge forming, and crash failure performance.

It is important noting that some AHSSs may exhibit significant differences between local ductility and crack propagation resistance. Therefore, when high damage tolerance and crack propagation resistance are a requirement, a fracture toughness-based rating should be favoured.

These observations highlight the relevance of carefully select the most appropriate material parameters to classify the overall formability and fracture resistance of AHSSs. The proposed classification concepts aim at providing useful guidelines for microstructural design and optimized material selection.

Acknowledgements

The present work has received funding from the European Union’s Research Fund for Coal and Steel programme under grant agreement No. 101112540 (Sup3rForm)

References

1. P. Larour, J. Freudenthaler, T. Weissböck: J. Phys.: Conf. Ser., **896**, 012073 (2017)
2. S. Heibel, T. Dettinger, W. Nester, T. Clausmeyer, A. E. Tekkaya: Materials, **11**, 761 (2018)
3. B. Hance: SAE Technical Paper 2018-01-0629, 2018, doi:10.4271/2018-01-0629.
4. I.A. Denks, M. Schneider, S. Westhäuser, C. Lesch. *Steel research int.*, **90** (2018)
5. G. Yim, J. Kim, J. Jeon, J. Hyun, B. M. Hance: IOP Conf. Ser.: Mater. Sci. Eng. **1307**, 012015(2024)
6. P.A.F. Martins, N. Bay; A.E. Tekkaya; A.G. Atkins. *Int. J. Mech. Sci.* **83**, 112 (2014)

7. M. Schneider, U. Eggers: *Proc. International Deep Drawing Research Group (IDDRG) 2011 conference*. Bilbao, Spain, June 5-8, 2011.
8. P. Larour, H. Pauli, J. Freudenthaler, J. Lackner, F. Leomann, G. Schestak: *Proc. International Deep Drawing Research Group (IDDRG) 2016 Conference*, Linz, Austria, June 12-15, 2016.
9. D. Frómeta, A. Lara, L. Grifé, T. Dieudonné, P. Dietsch, J. Rehrl, C. Suppan, D. Casellas, J. Calvo *Metall Mater Trans A* **52**, 840 (2021)
10. D. Frómeta, A. Lara, S. Molas, D. Casellas, J. Rehrl, C. Suppan, P. Larour, J. Calvo. *Eng. Frac. Mech.* **205**, 319 (2019)
11. Frómeta D, Cuadrado N, Rehrl J, Suppan C, Dieudonné T, Dietsch P, Calvo J and Casellas D *Mat. Sci. and Eng. A* **802**, 140631 (2021).
12. S. Golling, D. Frómeta, D. Casellas, P. Jonsén: *Mat. Sci. and Eng. A*, **743**, 529 (2019).
13. B. Cotterell, J.K. Reddel: *Int. J. Fract.* **13**, 267 (1977).
14. CWA 17793:2021. Test method for determination of the essential work of fracture of thin ductile metallic sheets
15. F. Hisker, R. Thiessen, T. Heller. *Mater. Sci. Forum* **706**, 925 (2012)
16. P. Jacques, Q. Furnémont, T. Pardoën, F. Delannay. *Acta Mater* **49** 139 (2001).